The Conformation of the Ribonucleic Acid in Ribsomes. Dye Stacking Studies*

A. V. Furano, D. F. Bradley, and L. G. Childers

ABSTRACT: Spectrophotometric titrations indicate that acridine orange binds to approximately 90% of the ribonucleic acid (RNA) phosphates in intact ribosomes of *Escherichia coli*. The dye binds rapidly, reaches an equilibrium distribution among binding sites within 30 sec, and is displaced by stoichiometric amounts of polylysine. The amount of dye bound is independent of the protein content of various ribosome preparations. The spectrum of the bound dye in a 1/1 dye–ribosome complex is metachromatic, indicative of interaction between dyes (*i.e.*, dimer formation) on adjacent binding sites of the ribosome. As the polymer (ribosome) to dye ratio (P/D) is increased, the bound dye spectrum becomes orthochromatic indicating that the dyes redistribute among the binding sites so that some dyes occupy sites with empty sites as neighbors. This variation of the dye spectrum with P/D is reflected in a change of the extinction of the dye at 504 mμ and can be quantitated by two parameters, $d\epsilon_{504}/d(P/D)$, and a constant, K.

Previous studies on the binding of acridine orange to other polynucleotides have shown that whenever the polymer is double helical, $d\epsilon/d(P/D)$ is high and K is low. Conversely, acridine orange complexes with polymers that have less ordered configuration show a low $d\epsilon/d(P/D)$ and high K. Comparison of these parameters for the binding of acridine orange to ribosomes, isolated ribosomal RNA, soluble RNA, and formylated ribosomal RNA leads to the conclusion that RNA in the ribosomes has little double-helical character, much less, in fact than isolated ribosomal RNA. A model of ribosomal structure based on the idea that the RNA in the ribosome has little double-helical character is presented and discussed.

The mechanism of ribosomal action in protein synthesis is poorly understood. Part of this lack of understanding is due to our ignorance as to the details of ribosomal structure. It is commonly believed that ribosomal ribonucleic acid (RNA) in the ribosome and isolated ribosomal RNA in aqueous solution have very similar conformations with appreciable double-helical character. The evidence for this assumption is the similarity of hypochromisms (Schlessinger, 1960; Hall and Doty, 1959) and X-ray powder diffraction patterns (Zubay and Wilkins, 1960; Klug *et al.*, 1961) of ribosomes and isolated ribosomal RNA.

Recently, Morgan and Rhoads (1965) showed that AO[1] binds to yeast ribosomes and that the amount of dye bound was equal to 50–80% of the ribosomal RNA phosphates. Bradley and co-workers (Bradley and Wolf, 1959; Bradley and Felsenfeld, 1959; Stone and Bradley, 1961) had previously shown that the change in the spectrum of the bound dye with increasing polynucleotide/dye ratio was related to the amount of double-helical content of the polynucleotide. On the basis of a comparison of the spectral changes in the ribosome–AO and DNA–AO complexes, Morgan and Rhoads concluded that ribosomal RNA is much more flexible, *i.e.*, has less double-helical content, than native deoxyribonucleic acid (DNA).

Comparison of the spectral changes obtained for ribosome–AO by Morgan and Rhoads with those obtained in our laboratory (Bradley and Felsenfeld, 1959) for RNA–AO complexes indicated that RNA in the yeast ribosome has much less helical content than isolated soluble ribonucleic acid (s-RNA) and ascites tumor RNA. We were then led to the question of whether the RNA in intact ribosomes has less double-helical content than isolated ribosomal RNA and/or whether it has any significant amount of double-helical content. We have, therefore, studied the spectral parameters of complexes between AO and ribosomes, isolated ribosomal RNA, and formylated ribosomal RNA, the latter taken as a model of nondouble-helical RNA. The results obtained lead to the conclusion that the RNA in the ribosome has very little double-helical content, about comparable to that present in extensively formylated RNA, and much less than isolated ribosomal RNA. A model of ribosomal structure incorporating a nondouble-helical RNA is proposed which appears to be consistent with the X-ray and hypochromicity studies cited above. The model is particularly well suited to explain many of the physical properties of ribosomes as well as the role of ribosomal RNA in the formation of ribosome–messenger ribonucleic acid (m-RNA)–aminoacyl s-RNA complexes.

* From the National Institute of Arthritis and Metabolic Diseases and the National Institute of Mental Health, National Institutes of Health, Bethesda, Maryland 20014. *Received April 8, 1966.*

[1] Abbreviation used: AO, acridine orange.

Methods

Ribosomes. The isolation of ribosomes from *Escherichia coli* B as well as their chromatography on DEAE-cellulose has been described elsewhere (Furano, 1966). The method of preparation of mammalian ribosomes was similar to that described by Wettstein *et al.* (1963). The livers of male rats that had been fasted overnight were homogenized in 3 volumes of a buffer containing 0.01 M Tris–HCl, pH 7.4, 0.001 M magnesium acetate, 0.025 M KCl, and 0.25 M sucrose. After the nuclei and unbroken cells were removed by centrifugation for 10 min at 1000*g* the homogenate was centrifuged for 30 min at 30,000*g*. To the upper four-fifths of the supernatant material was added 15 mg of deoxycholate/ml, and the mixture (7 ml) was layered on a discontinuous sucrose gradient consisting of a layer (3 ml) of 0.5 M sucrose and a lower layer (3 ml) of 2.0 M sucrose, both of which contained 0.01 M Tris–HCl, pH 7.4, and 0.001 M magnesium acetate. The tubes were centrifuged for 3 hr at 105,000*g* (40,000 rpm) and the supernatant material was discarded. The tubes were wiped dry and the ribosomal pellet was resuspended in a small amount of 0.01 M Tris–HCl, pH 7.4, containing 0.0001 M magnesium acetate and dialyzed for 12 hr against 1 l. of the same buffer. The ribosomes contained 53% RNA and 47% protein.

RNA. E. coli B s-RNA (General Biochemicals, Inc.) was purified before use according to the method of von Ehrenstein and Lipman (1963). *E. coli* B ribosomal RNA was prepared from ribosomes by a method similar to that of Kurland (1960) and Littauer and Eisenberg (1959). Sodium dodecyl sulfate was added to a suspension of ribosomes (1 mg/ml) in 0.01 M Tris–HCl, pH 7.4, 0.001 M EDTA to give final concentration of 0.2 mg/ml. After 5 min at room temperature, an equal volume of phenol was added to the suspension and the mixture was stirred at room temperature for 1 hr. The mixture was centrifuged for 5 min at 10,000*g*, the aqueous phase was removed, and the phenol layer was washed with 0.5 volume of 0.01 M Tris, pH 7.4, containing 0.001 M EDTA. The pooled aqueous layers were extracted with 0.5 volume of fresh phenol which was then removed by centrifugation and discarded. Absolute ethanol (2 volumes) was added to the aqueous layer and the RNA was collected by centrifugation after 1.5 hr at 0°. The RNA was reprecipitated, dissolved in the above buffer, and dialyzed for 12 hr against 2 l. of 0.01 M Tris–HCl, pH 7.4. The solution of RNA (1 mg/ml) was stored at −20°.

Assays. RNA was determined by pentose analysis (Schneider, 1957) and protein was measured according to the method of Zamenhof (1957). Phosphate analysis was carried out as described by Ames and Dubin (1960). Lipid phosphate was removed from mammalian ribosomes by incubating lyophilized ribosomes with 20 volumes of chloroform–methanol (2/1, v/v) for 2 hr at room temperature. The lipid-free residue was removed from the chloroform–methanol by centrifugation, dried under an air stream, and dissolved by heating for 3 min at 70° in 0.1 ml of 0.1 M KOH.

Dye binding and stacking experiments as well as the purification of the AO (Chroma-Gesellschaft) were carried out as described previously (Stone and Bradley, 1961). Poly-L-lysine of reported mol wt 40,000–60,000 (Schwartz Bioresearch) was used as supplied.

Results and Discussion

1. Spectrophotometric Titrations. The binding of AO to polynucleotides is accompanied by spectral changes of the dye which are dependent on the ratio of dye to binding sites (*i.e.*, phosphates) of the polynucleotide. As a solution of AO is titrated with a given polynucleotide the α band (492 mμ) of the free dye diminishes and a β band at *ca.* 464 mμ (or a γ band with some polyanions at *ca.* 440 mμ) increases in intensity. Beyond a certain point, further addition of polynucleotide causes the β band to diminish and the α band to reappear but at a new wavelength *ca.* 504 mμ. The changes produced in the spectrum of AO (also seen when the dye is titrated with polyanions other than polynucleotides) which has been titrated with ribosomal RNA, ribosomes, formylated ribosomal RNA, DNA, and s-RNA are illustrated in Figures 1 and 2. Curve H in Figure 1A is the spectrum of the free dye. Curves A in Figures 1A–F represent the spectra of approximate 1/1 dye–polynucleotide complexes and curves B–G represent the effect of increasing ratios of polymer to dye (P/D) on the spectrum of the bound dye. It is apparent that the changes in the spectrum of AO are qualitively the same for all of the polynucleotides used including ribosomes. As can be seen in Figure 2, these spectral changes in AO can be conveniently followed by observing the change in the extinction of the dye at 504 mμ as a function of the amount of polymer added to the dye. Two features of these titration curves, which will be discussed below in detail, should be noted. (A) A sharp end point (defined as the intersection of the two linear limbs of the titration curve) is seen in all the titration curves as polymer is added to the dye. (B) There are obvious differences between the polymers in the slopes $[d\epsilon_{504}/d(P/D)]$ of the right-hand limbs of the titration curves. Thus, although the spectrum of AO undergoes the same kind of change regardless of what polymer is used, there are marked differences among the polymers in their ability to increase the extinction of the dye at 504 mμ from its minimum (*cf.* Figures 1 and 2) as excess polymer is added to the dye.

A. STOICHIOMETRY AT THE TITRATION END POINT. Previous studies (Bradley and Wolf, 1959; Bradley and Felsenfeld, 1959; Stone and Bradley, 1961) have shown that the end point of the spectrophotometric titration, defined as the intersection of the two linear limbs of the titration curve (see Figure 2), corresponds to the formation of 1/1 complexes between the dye and the polynucleotide phosphates. The phenomenon is not restricted to polynucleotides, as many polyanions have been shown to form 1/1 complexes with AO and other metachromatic dyes at corresponding titration end points (*cf.* Stone *et al.*, 1963). By measur-

TABLE I: Stoichiometry.[a]

No.	RNA/ Protein	Buffer (M) Stock	Buffer (M) Titration	RNA Phosphate ($\times 10^3$ M)	Vol. of RNA at End Point (μl)	Moles of RNA Phosphate at End Point ($\times 10^9$)	Moles of AO at End Point ($\times 10^9$)	% RNA Phosphate Titrated	HCHO
			E. coli Ribosomes						
6/16	60/40	10^{-3} P 10^{-4} Mg^{2+}	10^{-3} C 10^{-4} Mg	1.80*	24.8	44.5	41.9	93	
10/15	60/40	10^{-3} P 10^{-4} Mg^{2+}	10^{-3} C 10^{-4} Mg	2.18*	25.0	54.4	43.9	81	
7/27	70/30	10^{-3} P 10^{-4} Mg^{2+}	10^{-3} C 10^{-4} Mg	2.62*	17.7	46.4	43.4	94	
10/8	70/30	10^{-3} P 10^{-4} Mg^{2+}	10^{-3} C 10^{-4} Mg	2.62	18.5	48.5	43.1	89	
12/3	60/40	10^{-2} Tris 10^{-4} Mg^{2+}	10^{-3} C 10^{-4} Mg	1.77	27.2	48.1	45.5	95	
12/22	60/40	10^{-2} Tris 10^{-3} Mg^{2+}	10^{-3} C 10^{-3} Mg	1.78*	28.9	51.4	44.8	87	
1/27	70/30	10^{-2} Tris 10^{-4} Mg^{2+}	10^{-3} C 10^{-4} Mg	1.63	28.8	46.9	43.3	92	
4/27	60/40	10^{-3} P 10^{-4} Mg^{2+}	10^{-3} C 10^{-4} Mg	1.75*	24.5	42.9	42.2	98	1%, $t = 0$
6/15	60/40	10^{-3} P 10^{-4} Mg^{2+}	10^{-3} C	1.80*	25.5	45.9	42.4	92	
10/18	60/40	10^{-3} P 10^{-4} Mg^{2+}	10^{-3} C	2.18*	25.0	54.4	43.8	81	
7/28	70/30	10^{-3} P 10^{-4} Mg^{2+}	10^{-3} C	2.62*	18.3	47.9	43.0	90	
11/9	60/40	10^{-2} Tris 10^{-4} Mg^{2+}	10^{-3} C	1.77	29.0	51.3	46.2	90	
6/1	60/40	10^{-3} P 10^{-4} Mg^{2+}	10^{-3} C	1.80*	25.5	45.9	43.8	95	
4/22	60/40	10^{-2} Tris 10^{-4} Mg^{2+} 20% sucrose	10^{-3} C 20% sucrose	1.72	31.1	53.5	43.1	81	

[a] Stoichiometry between acridine orange and polynucleotide phosphates at titration end points (see text and legend to Figure 2). The dates on which the experiments were carried out are listed in column one to facilitate comparison of Tables I and II. The second column indicates the type of ribosome preparation used, *i.e.*, 60/40 RNA/protein ratio are ribosomes prepared by repeated centrifugation and which contain on the average 40% protein by weight; 70/30 RNA/protein ratio are ribosomes further purified by chromatography on DEAE-cellulose (see Methods) and contain on the average 30% protein by weight. The 53/47 RNA/protein ratio are rat liver ribosomes and contained 47% protein by weight. The third column lists the components of the buffers in which the samples were stored before titration. 10^{-3} P, 10^{-2} Tris, and 10^{-4} Mg^{2+} correspond to 10^{-3} M potassium phosphate, pH 7.0, 10^{-2} M Tris–Cl, pH 7.4, and 10^{-4} M magnesium acetate. The fourth column lists the components of the media in which the titra-

ing the amounts of dye and polynucleotide phosphate at the titration end points, it is possible to determine the fraction of the phosphates which are available to bind AO.

The stoichiometries at the titration end points are shown in Table I. It can be seen that the number of binding sites corresponds closely to the number of phosphate groups for ribosomes as well as s-RNA and ribosomal RNA. For *E. coli* ribosomes, the per cent of phosphates titrated ranges from 81 to 95 with a mean value of 90%, excluding the values obtained from titrations carried out in 1% formaldehyde (98%), 20% sucrose (81%), and 10^{-3} M Mg^{2+} (87%).

The following evidence supports the conclusion

TABLE I: (*Continued*)

No.	RNA/ Protein	Buffer (M) Stock	Buffer (M) Titration	RNA Phosphate ($\times 10^3$ M)	Vol. of RNA at End Point (μl)	Moles of RNA Phosphate at End Point ($\times 10^9$)	Moles of AO at End Point ($\times 10^9$)	% RNA Phosphate Titrated	HCHO
			Rat Liver Ribosomes						
1/25	53/47	10^{-2} Tris	10^{-3} C	0.97	58.0	56.3	43.6	77	
		10^{-4} Mg^{2+}	10^{-4} Mg	(0.775)		(45.0)		(97)	
			E. coli Ribosomal RNA						
12/11	...	10^{-3} P	10^{-3} C	2.84	15.5	44.0	46.0	105	
		10^{-4} Mg^{2+}							
6/21	...	10^{-3} P	10^{-3} C	2.31*	18.6	43.0	42.3	98	
6/1	...	10^{-3} P	10^{-3} C	2.95*	14.4	42.5	43.3	102	
8/19	...	10^{-3} P	10^{-3} C	2.92*	14.8	43.2	41.6	96	
3/17	...	10^{-3} P							
		100°/30 min	10^{-3} C	5.49*	8.3	45.6	43.8	96	
10/13	...	10^{-3} P	10^{-3} C	2.87*	16.1	46.2	44.0	95	
		10^{-4} Mg^{2+}	10^{-4} Mg^{2+}						
3/11	...	10^{-3} P	10^{-3} C	2.87*	15.4	44.2	43.5	98	1%, t = 0
4/12	...	10^{-3} P	10^{-3} C	2.87*	17.4	49.9	42.4	85	1%, t = 0
5/28	...	10^{-3} P	10^{-3} C	2.87*	14.8	42.5	44.0	104	1%, 24 hr
3/26	...	10^{-3} P	10^{-3} C	2.60*	16.3	42.4	44.0	104	5%, 24 hr
6/22	...	10^{-3} P	10^{-3} C	2.60*	18.0	46.8	43.0	92	5%, 24 hr
6/4	...	10^{-3} P	10^{-3} C	2.60*	16.5	42.9	42.9	100	5%, 72 hr
4/7	...	10^{-3} P	10^{-3} C	2.32*	26.5	61.5	42.4	69	10%, 24 hr
3/24	...	10^{-3} P	10^{-3} C	5.47*	9.5	52.0	42.6	82	10%, 100°/ 30 min
			E. coli B s-RNA						
12/24	...	10^{-2} Tris	10^{-3} C	3.40	13.2	44.8	45.2	101	
		10^{-4} Mg^{2+}							
6/17	...	10^{-3} P	10^{-3} C	3.11*	13.3	41.4	41.8	101	
8/18	...	10^{-3} P	10^{-3} C	2.33*	19.5	45.4	41.9	92	
4/8	...	10^{-3} P	10^{-3} C	2.99	12.5	37.4	43.0	115	5%, 24 hr

tion was carried out. 10^{-3} C corresponds to 10^{-3} M sodium cacodylate buffer, pH 6.7. In column five are the molarities of the ribosomal or RNA phosphates. The unstarred values were determined by direct phosphate analysis (see Methods), whereas the starred values were determined from the ϵ_{260} of the polymers, *i.e.*, 8000, 8290, 7450, and 7060 for the 60/40 ribosomes, the 70/30 ribosomes, ribosomal RNA, and s-RNA, respectively. In column six are the volumes of polymer added to reach the titration end point (see text and legend to Figure 2), in column seven are the total amounts of polymer phosphate added at the end point and in column eight are the total amounts of AO in the titration media. The last column gives the conditions under which certain samples were treated with formaldehyde before titration. Per cents are given in w/w and times (t) in hours. The titration media always contained the same concentration of formaldehyde as that with which the sample had been pretreated.

that only the RNA phosphates of the ribosome bind the dye. (1) As mentioned above, there is a close correlation between the number of RNA phosphates and dyes bound. (2) There is no apparent correlation between the number of dye binding sites and the protein content of the ribosomes. The mean values of the percentage of phosphates titrated for *E. coli* ribosomes containing on the average 40% w/w protein is 90% and for *E. coli* ribosomes that had been purified on DEAE-cellulose and which contained on the average 30% w/w protein is 91%. Furthermore, it is unlikely that the dye displaces protein which is normally bound to RNA phosphates. Thus, experiments with ribosomes (40% w/w protein) whose protein was uniformly labeled with [^{14}C]leucine showed that only 8% of the radioactivity was released into solution when a 1/1 dye–ribosome complex was made.

For rat liver ribosomes containing 47% w/w protein,

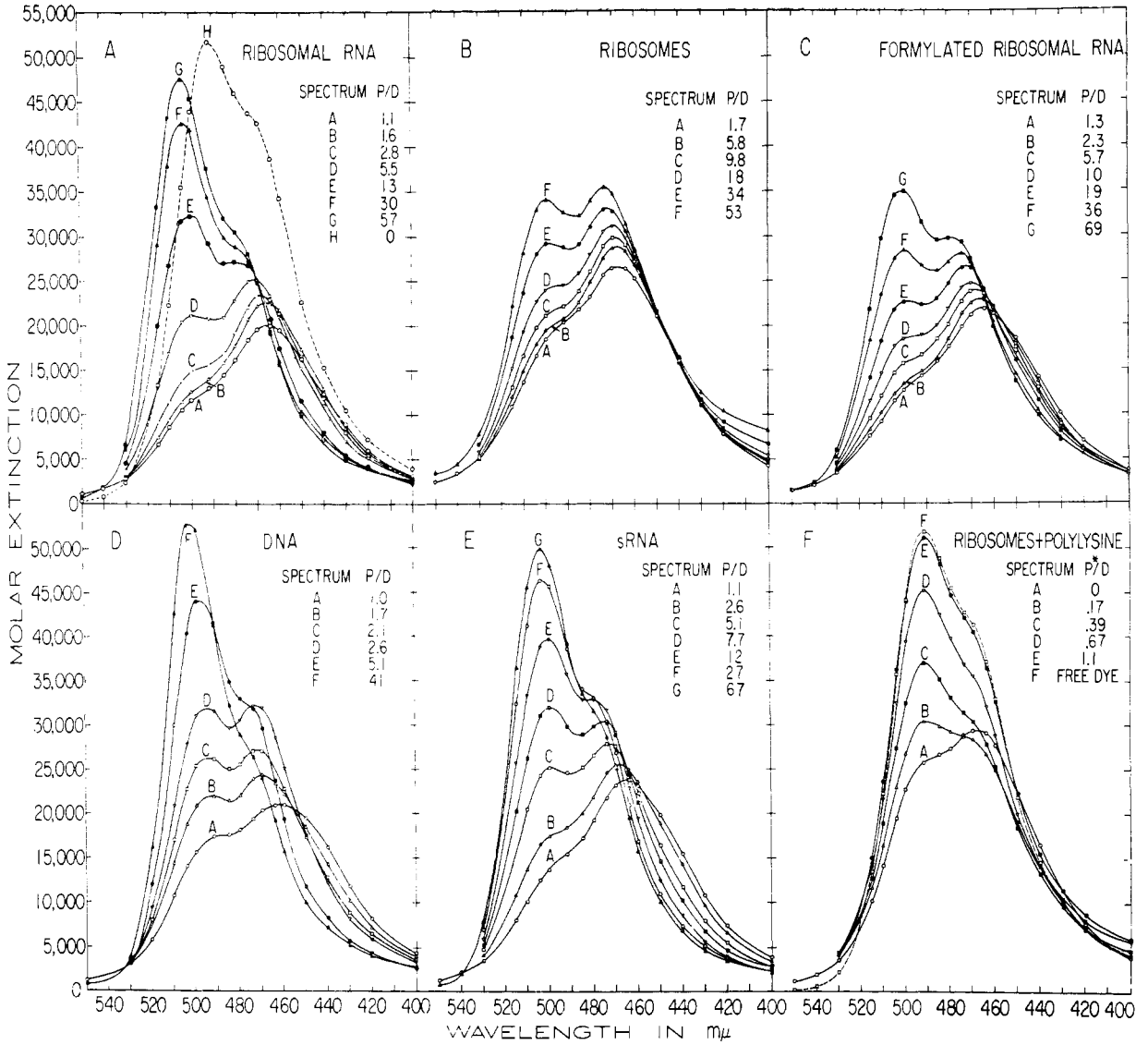

FIGURE 1: Spectra of acridine orange bound to ribosomes and polynucleotides. Ordinate: molar extinction coefficient of acridine orange. P/D is polymer to dye ratio; P*/D is polylysine to dye ratio. Curve H of Figure 1A is the spectrum of the free dye at approximately 1×10^{-5} M in 1×10^{-3} M sodium cacodylate buffer, pH 6.7, at 25°. All other curves in Figures 1A–E are spectra of acridine orange (10^{-5} M in the cacodylate buffer) bound to the designated polymers at the indicated P/D (for details of a typical titration see legend to Figure 2). The buffer in which the ribosomes were titrated contained 10^{-4} M magnesium acetate; the buffer in which the formylated ribosomal RNA (pretreated for 24 hr with 5% formaldehyde by weight at 25°) was titrated contained 5% formaldehyde by weight. Curve A of Figure 1F represents an approximate 1/1 dye–ribosome complex. Curves B–F of this figure correspond to the increasing amounts of dye displaced from the ribosome by polylysine, *e.g.*, curve C corresponds to a mixture of free and bound dye when 0.39 polylysyl cationic charges/ribosomal phosphate have been added; when 1 polylysyl charge/ribosomal phosphate have been added all of the dye is released and the spectrum (E) is that of the free dye (F).

the per cent of phosphates titrated is 77%. However, extraction of these ribosomes with chloroform–methanol removed 20% of the phosphates which presumably represent contaminating phospholipid. If it is assumed that the phospholipid does not have sufficient polyelectrolyte character (A. Stone, M. E. Lamm, and D. F. Bradley, in preparation) to bind AO, then 97% of the RNA phosphates must be available for dye binding.

The per cent phosphates titrated with isolated ribosomal RNA ranged from 95 to 105% with a mean value of 99%. After treatment with 1 and 5% formaldehyde, the mean values were 96 and 99%. The single value in 10% formaldehyde was somewhat lower (69%). The mean value for *E. coli* s-RNA was 98%.

B. SPECTRAL CHANGES IN THE REGION OF POLYMER

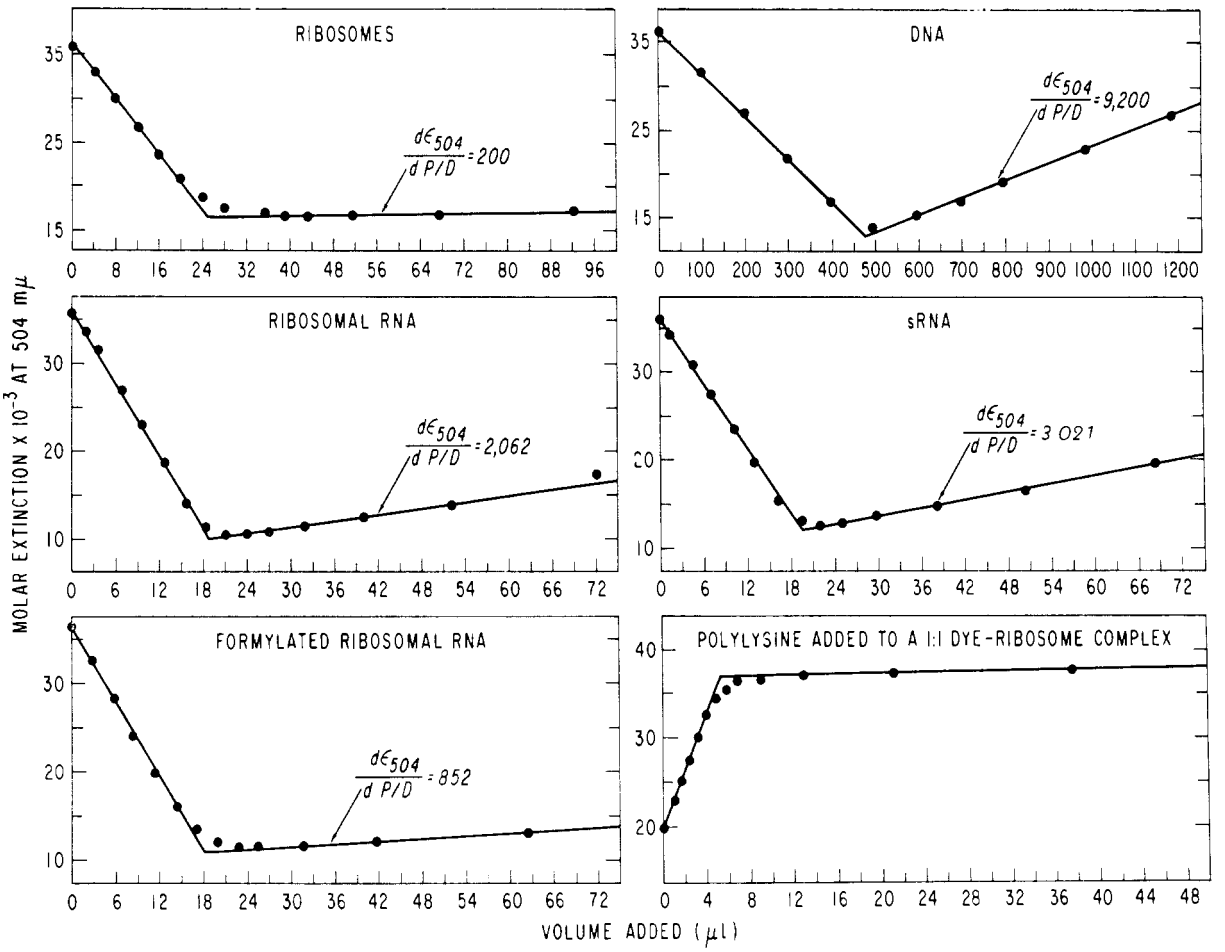

FIGURE 2: Spectrophotometric titration of acridine orange with ribosomes and polynucleotides. Ordinate: molar extinction at 504 mμ of acridine orange. Compositions of the buffers and the conditions of the titrations are same as described in legend to Figure 1. In a typical titration 4.8×10^{-8} mole of dye were contained in 2.4 ml of buffer in a 1-cm, glass-stoppered cuvet, stirred by a micromagnetic stirring bar. After each addition of polymer the solution was stirred 90 sec, weighed (±0.1 mg) to determine the exact volume of polymer added, and the spectrum was taken on a Model 14 Cary spectrophotometer. Throughout the descending limb of the titration curve the extinctions correspond to a mixture of free and polymer-bound dye. The dye is essentially completely bound at the point of minimum extinction or end point defined by the intersection of the two linear limbs of the titration curve. As excess polymer is added beyond this point, the fraction of dyes without neighbors (*i.e.*, monomers) increases causing the observed increase in extinction since 504 mμ corresponds to the absorption maximum of the bound monomer dye. The slopes $[d\epsilon_{504}/d(P/D)]$ are just the increases in extinction produced by increasing the amount of polymer to two times its value at the end point, and is an easily determined, convenient measure of the fraction of dyes with no neighbors that exists at equilibrium when one-half the polymer sites are occupied by the dye and one-half are empty. The bottom right-hand titration illustrates the effect of adding polylysine to a 1/1 dye–ribosome complex where the increase in extinction results from the displacement of the bound dye by polylysine. At a 1/1 equivalence of polylysyl and ribosomal phosphate charges all the dye is free in solution and further addition of polylysine does not affect the spectrum. The moles of AO in the above titrations as well as the molarities of the polymer phosphate are given in Table I; *i.e.*, ribosomes, no. 6/16; ribosomal RNA, no. 6/21; formylated ribosomal RNA, no. 6/22; s-RNA, no. 8/18. In the polylysine experiment a mixture of AO (45.2×10^{-9} mole) and ribosomes (46.6×10^{-9} mole of ribosomal phosphate) was titrated with a solution of polylysine (7.58×10^{-3} M cationic charges). The experiment with DNA (calf thymus, Sigma Chemical Co.) has been previously reported (Bradley and Felsenfeld, 1959; Stone and Bradley, 1961) and is included for comparison. In this titration 46.6×10^{-9} mole of AO was titrated with a solution of DNA that was 9.50×10^{-5} M in phosphate (calculated from an ϵ_{260} of 6200).

EXCESS. As was mentioned earlier, when polynucleotide is added to the dye in excess of a 1/1 ratio of dye to polynucleotide phosphate, the spectrum of the dye approaches a shape similar to that of the unbound dye, *i.e.*, the α band reappears but with a λ_{max} shifted to *ca.* 504 mμ. This phenomenom is illustrated in Figure 1, and the increase in extinction at 504 mμ (*i.e.*, reappearance of the α band) when plotted as a function

TABLE II: Dye Stacking Parameters.[a]

No.	RNA/ Protein	Buffer (M) Stock	Buffer (M) Titration	$\epsilon_{504} \times 10^{-3}$ min	$\epsilon_{504} \times 10^{-3}$ max	$d\epsilon_{504}/d(P/D)$ ($\times 10^{-2}$)	Stacking Coeff, K	HCHO
			E. coli Ribosomes					
6/16	60/40	10^{-3} P, 10^{-4} Mg	10^{-3} C, 10^{-4} Mg	16.7	33.0 (53)	2.0	48 ± 5	
10/15	60/40	10^{-3} P, 10^{-4} Mg	10^{-3} C, 10^{-4} Mg	16.7	29.9 (51)	3.3	69 ± 5	
7/27	70/30	10^{-3} P, 10^{-4} Mg	10^{-3} C, 10^{-4} Mg	16.3	31.9 (74)	2.0	79 ± 7	
10/8	70/30	10^{-3} P, 10^{-4} Mg	10^{-3} C, 10^{-4} Mg	16.2	33.9 (67)	4.8	55 ± 4	
6/15	60/40	10^{-3} P, 10^{-4} Mg	10^{-3} C	15.3	34.3 (50)	6.2	40 ± 3	
10/18	60/40	10^{-3} P, 10^{-4} Mg	10^{-3} C	15.3	29.8 (50)	5.2	55 ± 2	
7/28	70/30	10^{-3} P, 10^{-4} Mg	10^{-3} C	15.2	33.0 (66)	6.5	51 ± 3	
6/1	60/40	10^{-3} P, 10^{-4} Mg	10^{-3} C	14.7	...	6.7	...	
4/27	60/40	10^{-3} P, 10^{-4} Mg	10^{-3} C, 10^{-4} Mg	16.4	29.9 (51)	2.4	74 ± 9	1%, t = 0
12/3	60/40	10^{-2} T, 10^{-4} Mg	10^{-3} C, 10^{-4} Mg	17.1	39.5 (45)	6.4	28 ± 7	
12/22	60/40	10^{-2} T, 10^{-3} Mg	10^{-3} C, 10^{-3} Mg	20.8	40.8 (39)	3.0	22 ± 5	
1/27	70/30	10^{-2} T, 10^{-4} Mg	10^{-3} C, 10^{-4} Mg	15.7	37.8 (45)	8.1	28 ± 6	
11/9	60/40	10^{-2} T, 10^{-4} Mg	10^{-3} C	15.4	38.9 (42)	8.5	21 ± 4	
4/22	60/40	20% sucrose, 10^{-2} T, 10^{-4} Mg	20% sucrose, 10^{-3} C	18.0	43.0 (40)	2.4	16 ± 5	
			Rat Liver Ribosomes					
1/25	53/47	10^{-2} T, 10^{-4} Mg	10^{-3} C, 10^{-4} Mg	17.8	32.4 (23)	6.7	26 ± 4	
			E. coli Ribosomal RNA					
12/11	...	10^{-2} T, 10^{-4} Mg	10^{-3} C	12.1	49.0 (80)	23	7.8 ± 1	
6/21	...	10^{-3} P	10^{-3} C	10.6	47.5 (57)	21	7.2 ± 1	
6/1	...	10^{-3} P	10^{-3} C	12.1	...	22	...	
8/19	...	10^{-3} P	10^{-3} C	12.0	...	23	...	
10/13	...	10^{-3} P, 10^{-4} Mg	10^{-3} C, 10^{-4} Mg	12.4	50.6 (82)	24	7.5 ± 1	
3/17	...	10^{-3} P, 100°/30 min	10^{-3} C	12.0	49.4 (94)	19	12 ± 2	
3/11	...	10^{-3} P	10^{-3} C	12.3	48.9 (81)	20	9.3 ± 2	1%, t = 0
4/12	...	10^{-3} P	10^{-3} C	11.1	48.0 (72)	19	8.0 ± 1	1%, t = 0
5/28	...	10^{-3} P	10^{-3} C	11.7	46.3 (83)	17	12 ± 1	1%, 24 hr
3/26	...	10^{-3} P	10^{-3} C	14.2	37.8 (58)	8.2	28 ± 4	5%, 24 hr
6/22	...	10^{-3} P	10^{-3} C	11.5	34.4 (69)	8.5	38 ± 2	5%, 24 hr
6/4	...	10^{-3} P	10^{-3} C	11.8	34.5 (75)	7.5	40 ± 2	5%, 72 hr
4/7	...	10^{-3} P	10^{-3} C	20.3	33.3 (23)	8.6	31 ± 3	10%, 24 hr
3/24	...	10^{-3} P	10^{-3} C	13.1	40.6 (67)	16.2	19 ± 1	1%, 100°/30 min
			E. coli s-RNA					
12/24	...	10^{-2} T, 10^{-4} Mg	10^{-3} C	12.5	53.2 (90)	30	4.9 ± 1	
6/17	...	10^{-3} P	10^{-3} C	12.7	51.6 (96)	18	9.8 ± 3	
8/18	...	10^{-3} P	10^{-3} C	12.6	49.8 (67)	30	4.3 ± 1	
4/18	...	10^{-3} P	10^{-3} C	15.7	45.0 (77)	8.3	18 ± 3	5%, 24 hr
			Yeast RNA					
2/19	...	10^{-3} C	10^{-3} C	12.0	48.5 (64)	36	6.0 ± 0.4	
8/16	...	10^{-3} C	10^{-3} C	11.4	...	40	...	
3/24	...	10^{-3} C	10^{-3} C	11.3	47.5 (59)	37	6.1 ± 0.4	0.1%, t = 0
3/12	...	10^{-3} C	10^{-3} C	10.9	40.0 (60)	12	20 ± 4	1%, t = 0
5/26	...	10^{-3} C	10^{-3} C	11.7	28.9 (56)	4	67 ± 7	5%, 24 hr
			Ascites Tumor RNA					
11/24	...	10^{-3} C	10^{-3} C	11.4	50.2 (61)	44	3.2 ± 0.6	
3/15	...	10^{-3} C	10^{-3} C	11.0	48.4 (60)	25	8.7 ± 1	1%, t = 0

[a] Numbers and symbols for the first four columns and column nine are the same as for Table I. Column five gives the extinction coefficient of the bound dye at 504 mμ at the end point of the titration ($\epsilon_{1/1}$). Column six gives the extinction of the bound dye at the highest polymer to dye ratio examined, *i.e.*, at the conclusion of the titration. The corresponding polymer to dye ratios are given in parenthesis. The seventh column is the slope of the ascending, right-hand limb of the titration curve (Figure 2). Column eight gives stacking coefficients (K) computed from eq 1 of the text. K is determined by fitting observed extinction (ϵ) and polymer dye ratios (P/D), using the values in column five for $\epsilon_{1/1}$ and $\epsilon = 55.0 \times 10^3$ for $\epsilon_{\infty/1}$, *i.e.*, the extinction of the bound dye at infinite polymer excess.

of the amount of polymer added to the dye produces the titration curves illustrated in Figure 2. It is in the region of polymer excess that the differences between various polynucleotides are revealed. More specifically, the slopes of the right-hand limb of the titration curve [*i.e.*, $d\epsilon_{504}/d(P/D)$, where P/D is the volume of polymer added/volume of polymer at the end point] are different for different polynucleotides.

At P/D values $>\sim 3$, ϵ_{504} is not a simple linear function of P/D. It has been possible, however, to express the entire ϵ_{504} *vs.* P/D titration curve in terms of a single parameter K by the relation (Geisser and Bradley, 1962).

$$\frac{\epsilon - \epsilon_{1/1}}{\epsilon_\infty - \epsilon_{1/1}} = \frac{2\left(1 - \frac{D}{P}\right)^2}{1 + 2(K-1)\frac{D}{P}\left(1 - \frac{D}{P}\right) + \left[1 + 4(K-1)\frac{D}{P}\left(1 - \frac{D}{P}\right)\right]^{1/2}} \quad (1)$$

where ϵ is the extinction at 504 mμ of the bound dye, $\epsilon_{1/1}$ is the extinction at 504 mμ of a 1/1 dye–polymer complex, and ϵ_∞ is the extinction of the dye–polymer complex extrapolated to infinite P/D. Equation 1 was derived on the assumptions that (1) the bound dyes distribute among the available polymer sites in a thermodynamic equilibrium governed by a free energy of interaction, $\Delta F_{int} = -RT \ln K$, between dyes bound to adjacent sites and (2) dyes with neighbors absorb maximally at 464 mμ (β band) and those without absorb maximally at 504 mμ (α band). According to this interpretation, the differences in, for example, $d\epsilon_{504}/d(P/D)$, for different polyanions is not due to variations in mode or site of binding but to the free energy of interaction between dyes on neighboring sites.

Previous studies have shown that low values of K [and high values of $d\epsilon_{504}/d(P/D)$] are obtained with polynucleotides of high double-helical content. Thus, a K of 1.2 is obtained for native DNA [$d\epsilon_{504}/d(P/D) = 9200$]. On the other hand, K values of 161 and 109 are obtained for polyriboadenylic acid (poly-A) and polyribouridylic acid (poly-U) in their random coil forms (Bradley and Wolf, 1959). Furthermore, changes in the double-helical content of any given polymer are reflected by changes in K, *e.g.*, heat denaturation of DNA followed by rapid recooling increases K from 1.2 to >6 [decreases $d\epsilon_{504}/d(P/D)$ from 9200 to 6400] (Stone and Bradley, 1961); transfer of poly-A to acid solution where it takes on double-helical character decreases K from 161 to 17 (Bradley and Wolf, 1959); formation of a two-stranded helical complex from random coil poly-U ($K = 109$) and poly-A ($K = 161$) reduces K to 6 (M. K. Wolf and D. F. Bradley, unpublished data).

Values of $d\epsilon_{504}/d(P/D)$ (estimated from titration curves such as those in Figure 2) and values of K [calculated from eq 1 by a curve-fitting procedure described elsewhere (Stone and Bradley, 1961)] for the polynucleotide–AO complexes studied in the present work are listed in Table II. The values of K for *E. coli* ribosomes stored in 10^{-3} M phosphate buffer (pH 7) ranges from 40 to 79 with a mean value of 57. On the other hand for ribosomes stored in 10^{-2} M Tris buffer (pH 7.4) the range and mean of K are 21–28 and 25. This effect of Tris on K was also found by Morgan and Rhoads (1965) who showed that the K for yeast ribosomes [estimated from $d\epsilon_{504}/d(P/D)$] decreased if the concentration of Tris buffer in the titration medium was increased from 10^{-3} to 10^{-2} M. The K value for rat liver ribosomes (26 ± 4) in 10^{-2} Tris buffer was similar to that of the *E. coli* ribosomes in the same buffer. The mean value of $d\epsilon_{504}/d(P/D)$ for the ribosomes is 540.

The values of K and $d\epsilon_{504}/d(P/D)$ obtained with ribosomes are significantly different from those obtained with isolated ribosomal RNA. The range of K for three different preparations of ribosomal RNA was 7.2–7.8 with a mean value of 7.5. In contrast to the ribosomes, there was little difference between K values obtained with RNA stored in Tris and phosphate buffers. The mean value for $d\epsilon_{504}/d(P/D)$ was 2260, approximately four times that obtained with the ribosomes. The value of the dye stacking parameters obtained with isolated ribosomal RNA are close to those obtained with other RNA's (see Table II). Two freshly prepared samples of *E. coli* s-RNA gave K values of 4.9 and 4.3, respectively, in Tris and phosphate buffers while a sample stored at $-10°$ for 6 months gave a $K = 9.8$. A commercial yeast RNA which had been studied previously by Lamm *et al.* (1965) gave a K of 6.0 and a sample of ascites tumor RNA, also employed previously (Bradley and Felsenfeld, 1959) had a K of 3.2. It can be seen from Table II that the values of $d\epsilon_{504}/d(P/D)$ for these polynucleotides are consistent with those expected from the values of K obtained with them.

2. Interpretation of Results. A. DYE STACKING PARAMETERS OF RIBOSOMES. The difference between the values of K and $d\epsilon_{504}/d(P/D)$ obtained with ribosomes and those obtained with isolated ribosomal RNA strongly suggest that the conformation of ribosomal RNA when packaged into a ribosome is quite different from the conformation of isolated ribosomal RNA. More specifically, the high values of K (57) and low values of $d\epsilon_{504}/d(P/D)$ (540) indicate that the RNA in the ribosome has significantly less double-helical content then isolated ribosomal RNA [$K = 7.5$, $d\epsilon_{504}/d(P/D) = 2260$]. However, the RNA in the ribosome exists as a ribonucleoprotein and it is therefore important to show that values of K or $d\epsilon_{504}/d(P/D)$ obtained with ribosomes have the same physicochemical basis as they do with other polynucleotides and thus can be used as valid indicators of the conformation of the RNA in the ribosome. That the dye stacking parameters obtained with ribosomes are directly comparable with those obtained with other polynucleotides is supported by a number of observations. (a) As has been shown for polynucleotides, the stoichiometric evidence presented above indicate that the dye binds to the RNA

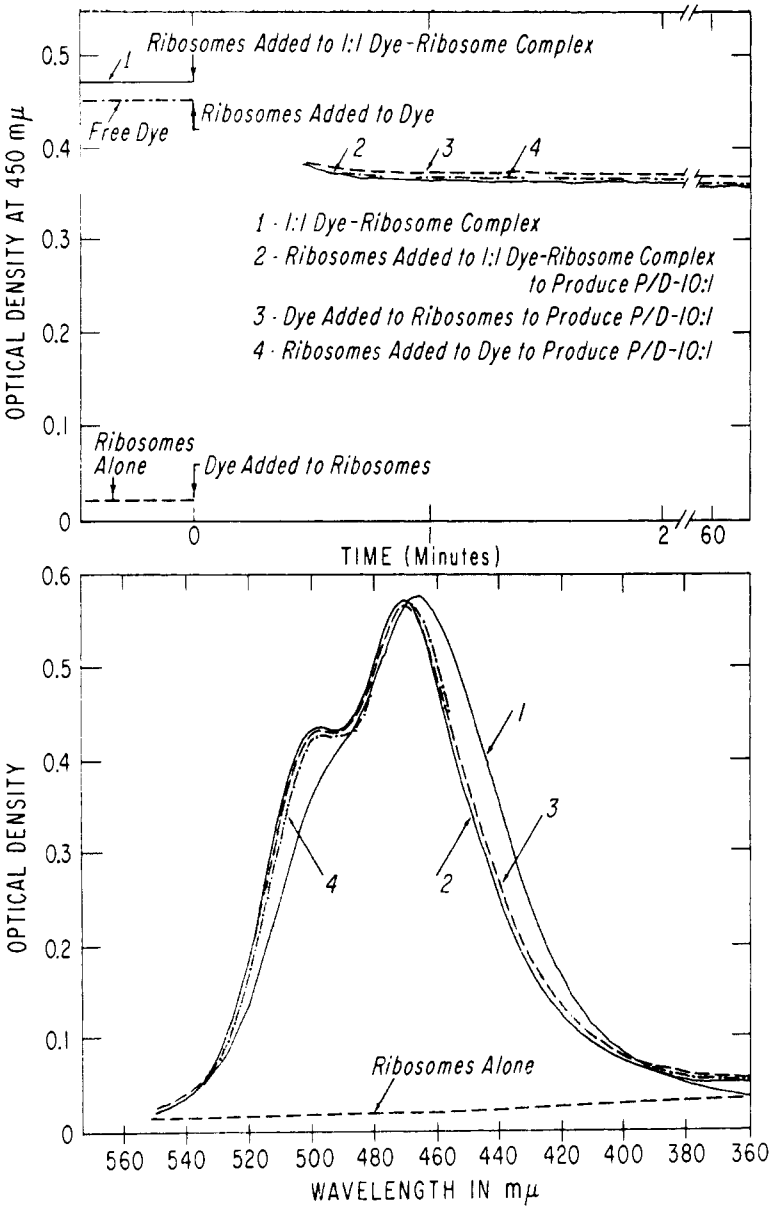

FIGURE 3: Kinetics of the binding and redistribution of acridine orange on ribosomes. Components and conditions of the titration mixtures were as described in legend to Figure 1. Upper figure: curve 1 (———) corresponds to the OD at 450 mμ of an approximately 1/1 dye–ribosome complex. At time zero (designated by arrow) sufficient ribosomes were added to give a final ribosome to dye ratio of 10/1 and the change in OD, curve 2, was recorded in the Cary spectrophotometer. (The gaps in the traces represent the time to make the various additions and reinsert the cuvet in the spectrophotometer.) In another trial dye was added to ribosomes (---------) to give a final ribosome of dye ratio of 10:1 and the change in OD was recorded (curve 3). In a final trial ribosomes were added to free dye (-·-·-·-) to produce a final ribosome to dye ratio of 10/1 and the change in OD was recorded (curve 4). As can be seen, the changes in OD are essentially complete by the time the recording is begun. Lower figure: the stationary-state spectra corresponding to the above trials are given.

nucleotides and not the protein (or contaminants such as phospholipid) of the ribosome. (b) The binding of the dye to the ribosomes is at least partially electrostatic as has been shown for other polynucleotides. Thus, the dye can be displaced from ribosomes by stoichiometric amounts of polylysine (av chain length 500) as is shown in Figure 1F and Figure 2. (c) The spectral changes of the dye bound to ribosomes are similar to those for the dye bound to other polynucleotides. Thus the λ_{max} and extinctions of the β band at P/D = 1 and of the α band as P/D is extrapolated to infinity of the dye bound to ribosomes are comparable to those obtained

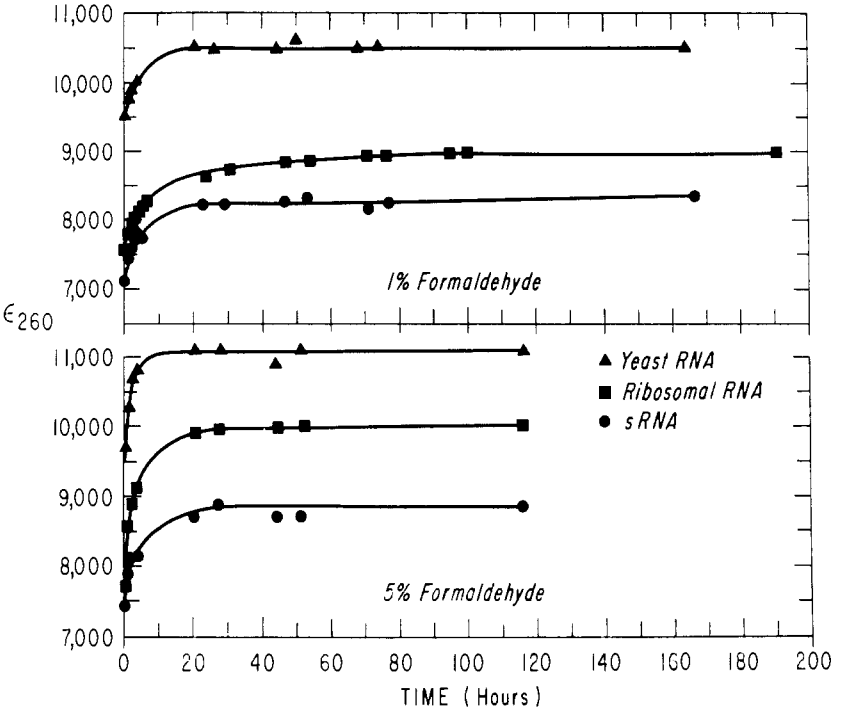

FIGURE 4: Reaction of formaldehyde with various ribonucleic acids. Ordinate: molar extinction coefficients of RNA's at 260 mμ. The values at zero time correspond to the extinctions of the RNA's at approximately 5×10^{-5} monomolar in 10^{-3} M sodium cacodylate buffer, pH 6.7. At time zero sufficient formaldehyde was added to the RNA in glass-stoppered cuvets to give either a 1 (upper curve) or 5% (lower curve) by weight formaldehyde solution. The reaction was continued at 25° for as long as 190 hr. There was negligible evaporation during this period (<1%).

with the dye bound to isolated ribosomal RNA and other RNA's (Figure 1, Table II). (d) As in the case of other polyanions, the spectrum of the dye obtained at any given P/D corresponds to an equilibrium distribution of dyes among binding sites on the ribosome. As shown in Figure 3, the same spectrum is achieved (1) by adding excess ribosomes to a 1/1 dye–ribosome complex, (2) by adding free dye to excess ribosomes, or (3) by adding excess ribosomes to free dye. These findings also demonstrate that the spectra achieved in the region of polymer excess is not dependent on the prior formation of a 1/1 ribosome–dye complex. Thus, it cannot be argued that the high values of K and the low values of $d\epsilon_{504}/d(P/D)$ represent merely a very slow rate of redistribution of the dyes among excess ribosomal binding sites as increasing amounts of polymer are added. Indeed, as shown in the upper part of Figure 3 where the spectral changes outlined above were followed as a function of time, it can be seen that the redistribution of dyes among excess sites is very rapid (<30 sec) as had been shown for other polynucleotides. It appears, therefore, that the mode of dye binding to ribosomes is similar to that for other polynucleotides and that the differences in K between ribosomes and isolated ribosomal RNA reflect the same factors which determine differences between the values of K for various RNA's and other polynucleotides, *i.e.*, double-helical content.

Although the mode of dye binding to ribosomes is similar to that for other polynucleotides, about 10% of the ribosomal phosphates are unavailable to bind the dye (see Table I) and it could be argued that the differences in K between the RNA in the ribosome and isolated ribosomal RNA may be only due to the blocking of some of the anionic charges of the RNA. To test this idea complexes of isolated ribosomal RNA and polylysine were titrated with AO. The values of the K's for complexes in which 0, 10, and 20% of the phosphates were blocked by polylysine were 6.6 ± 1.4, 6.2 ± 1.2, and 6.7 ± 1.5, respectively. These experiments are consistent with the idea that the mere blocking of some RNA phosphates by ribosomal protein is not sufficient in itself to account for the difference between the K of isolated ribosomal RNA and the RNA in the ribosome. Since the dye binding data indicate that, in contrast to isolated ribosomal RNA, the RNA in the ribosome has little or no double helical character it seems reasonable to conclude that the complexing of ribosomal protein to ribosomal RNA in some way holds the RNA in an essentially single-stranded structure.

B. FORMYLATION OF RNA. As discussed above, the high value of K (57) obtained with ribosomes as compared with the K (7.5) obtained with isolated ribosomal RNA indicates that the RNA in the ribosome has considerably less double-helical content

than isolated ribosomal RNA. If this conclusion is correct, one would expect that a decrease in the double-helical content of isolated ribosomal RNA should result in increased values of K for the isolated RNA. Treatment of RNA with formaldehyde, which reacts with amino groups on the nucleotide bases and interferes with hydrogen bonding between base pairs (Hall and Doty, 1959), should cause an increase in K with any RNA possessing appreciable helical character. In fact, Lamm *et al.* (1965) (see also Feder and Wolf, 1965) showed that formylation of yeast RNA does cause a marked increase in K.

Experiments were performed to determine the length of time required for the formaldehyde–RNA reaction to reach a stationary state as well as the extent of the reaction upon formaldehyde concentration. The course of the reaction (at 25°) was followed by the change in molar extinction of the RNA at 260 mμ (Figure 4). Both the rate and extent of reaction are greater in 5% HCHO than in 1% HCHO and after about 24 hr, no further optical changes occurred. The ϵ_{260} values at zero time were 7060, 7450, and 9360 for s-RNA, ribosomal RNA, and yeast RNA and the per cent increases at the steady state in 5% HCHO were 25, 37, and 19%, respectively. As can be seen from Tables I and II, the values of K for all RNA samples increase with HCHO treatment, although the number of binding sites for AO remains unaffected. The magnitude of the increase in K depends, as does ϵ_{260}, upon the length of treatment and concentration of HCHO (*cf.* Figure 4, Table II). After 24 hr in 5% HCHO, the K values for yeast RNA and s-RNA were 67 and 18, respectively. After a similar treatment, two preparations of ribosomal RNA had K values of 28 and 38 and prolongation of the HCHO treatment to 72 hr produced a maximum K of 40 for ribosomal RNA.

The above data illustrate again the dependence of K on the amount of double-helical character of the polynucleotide. More important, however, is the finding that extensively formylated ribosomal RNA, which should have little, if any, double-helical character, has values of K comparable to several of the lower values obtained with ribosomes in phosphate buffer. It would appear, therefore, that the RNA in ribosomes has as little or less double-helical content as does extensively formylated ribosomal RNA.

3. Relation of Dye Binding Results to Ribosomal Structure. The currently accepted model of the ribosome is based on the idea that ribosomal RNA has as much double-helical structure in the ribosome as in the isolated state. According to this view, the protein must be associated with the RNA in such a manner as to have little or no influence on the conformation of the RNA. The evidence upon which this model is based rests on (1) the similar hypochromicity of isolated ribosomal RNA and ribosomes (Schlessinger, 1960), (2) "melting" curves of ribosomal particles that are reminescent of isolated ribosomal RNA (Hall and Doty, 1959), and (3) similarity between X-ray diffraction patterns of wet gels of ribosomes and isolated ribosomal RNA (Zubay and Wilkins, 1960; Klug *et al.*, 1961).

On the other hand, the dye stacking data presented here indicate that the RNA in the ribosomes has much less helical content than isolated ribosomal RNA. In fact, the RNA in the ribosome has as little double-helical content as extensively formylated RNA. Further, the facts that most (90%) of the RNA phosphates can bind the dye, that the dyes distribute among excess binding sites at a rapid rate and that the dye can be replaced stoichiometrically by a large cation such as polylysine (av length 500) all point to a location of the nucleotide phosphates near or at the surface of the ribosomes and unblocked by ribosomal protein. Accordingly, we propose a model of the ribosome (Figure 5) in which the RNA is held in a single-stranded configuration by some kind of interaction between the nucleotide bases and the ribosomal protein and with the phosphates exposed to the solvent. The hypochromism and X-ray data used to support the earlier model of the ribosome are equally consistent with the model we are proposing. According to the theory of hypochromism developed by Tinoco (1960) and others (*e.g.*, DeVoe and Tinoco, 1962), any ordered array of nucleotides can exhibit hypochromism in the 260-mμ band, *i.e.*, hypochromism is a measure of the degree of ordering of bases and not of double-helical character.

In the model proposed here, van der Waals (*e.g.*, London dispersion) and electrostatic (*e.g.*, dipole–dipole) forces between nearest neighbor nucleotide bases along the single RNA strand in the ribosome could be sufficient to order the bases in stacks. Such stacking would not only account for the hypochromism exhibited by RNA in ribosomes but for the hyperchromism observed at elevated temperatures as the bases become unstacked and randomly oriented with respect to one another.

The X-ray diffraction studies of ribosomes were carried out with unoriented wet gels of ribosomes and ribosomal RNA which give essentially powder patterns. Such patterns cannot show the pattern of reflections that are characteristic of double-helical structures and thus are not able to reveal the presence of helicity in either ribosomal RNA or ribosomes. In fact, as was pointed out (Zubay and Wilkins, 1960; Klug *et al.*, 1961) a number of conformations of the RNA (*e.g.*, a single strand folded back on itself) are consistent with the X-ray data, especially since structural meanings cannot be assigned to the spacings obtained. Furthermore, even if such patterns could prove the existence of some double-helical RNA in the ribosome, they could not, without considerable further refinement of the measurements, determine the fraction of RNA in the ribosome which has double-helical character. The dye stacking measurements do not exclude the possibility that a small fraction of the RNA in the ribosome is double helical.

We feel that the model we are proposing is not only consistent with the physical evidence upon which other models for ribosomal structure are based, but also

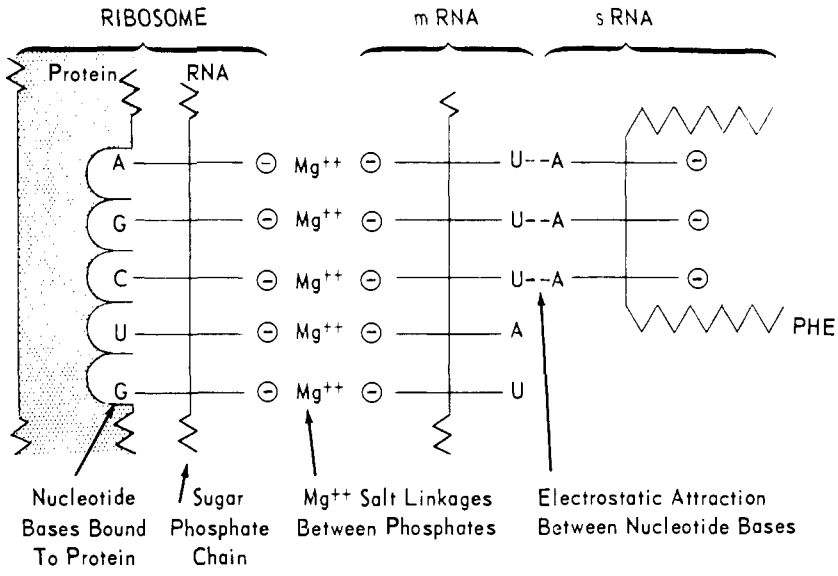

FIGURE 5: Model of ribosome binding m-RNA and aminoacyl s-RNA.

with a number of other observations that have been made about ribosomes. We should like to further develop our model in accord with these observations and point out some of the implications such a model would have for ribosomal function.

The strong dependence of the equilibrium between 30, 50, 70, and 100S ribosomal particles on Mg^{2+} (Tissiers *et al.*, 1959), coupled with the finding that in the 30 and 50S particles studied herein, 90% of the phosphates must be exposed to solvent leads to the suggestion that the above species are linked to one another by means of Mg^{2+} salt bridges between the RNA phosphates of the different particles.

The dependence upon Mg^{2+} of the binding of m-RNA to ribosomes (Spyrides and Lipman, 1962), suggests that, similarly, the phosphates of m-RNA are linked to the exposed phosphates of the ribosome *via* Mg^{2+} salt links as shown in Figure 5. In our model, the ribosome is, as a first approximation, a relatively nonspecific array of phosphates capable of binding an m-RNA of any base sequence. This is not to imply at all that other factors such as ribosomal protein, the tertiary structure of the ribosome, or enzymes that may bind to ribosomes, do not influence the interaction between ribosomes and m-RNA. If the m-RNA is bound to ribosomes as in Figure 5, it is obvious that the bases of the m-RNA are free to pair with anticodon bases of aminoacyl s-RNA.

Theoretical studies (Nash and Bradley, 1965; H. Nash and D. F. Bradley, in preparation) have indicated that the strength and specificity of interaction between codon and anticodon is highly dependent upon the geometric constraints imposed on them. As can be seen from Figure 5, the spatial relationships in the codon–anticodon complex will be determined at least in part by the arrangement of the ribosomal phosphates to which the m-RNA is bound and that changes in ribosomal conformation could change the reading of the genetic code. Alterations in ribosomal conformation may result from mutations affecting ribosomal RNA or ribosomal protein as well as from environmental factors. Perhaps the codon ambiguity produced by Mg^{2+} and other cations (So *et al.*, 1964; Szer and Ochoa, 1964) as well as such agents as streptomycin (Davies *et al.*, 1964; Pestka *et al.*, 1965) may indeed be mediated by the mechanisms suggested by the above model.

From the results presented in this paper we have concluded that whereas isolated ribosomal RNA contains considerable double-helical character, the RNA in the intact ribosome is as an essentially single-stranded structure. This conclusion differs from the interpretation of the results obtained with ribosomal studies of hypochromism, X-ray diffraction, and most recently, optical rotary dispersion (Blake and Peacocke, 1965). In spite of the similarities that we have demonstrated between the nature of AO binding to ribosomes and other polynucleotides one could argue that the experimentally determined relationship between K [and $d\epsilon/d(P/D)$] and double helicity of polynucleotides may not extend to protein–polynucleotide complexes such as ribosomes. However, one can also argue that the data obtained on hypochromism, X-ray defraction, and optical rotary dispersion are not inconsistent with a single-stranded conformation of the RNA in the ribosome. The most judicious conclusion at this point would be that the experimental evidence available cannot be viewed as sufficiently discriminatory to completely eliminate either a double-helical or a single-stranded conformation of the RNA in the intact ribosome. Nevertheless, we feel that the model we have proposed for nondouble-helical RNA in the ribosome to be worthy of serious consideration. Accordingly, it seemed desirable to speculate as to what might hold

the ribosomal RNA in such a conformation and what such a conformation would mean in terms of ribosomal structure and function in protein synthesis.

References

Ames, B. N., and Dubin, D. T. (1960), *J. Biol. Chem. 235*, 769.

Blake, A., and Peacocke, A. R. (1965), *Nature 208*, 1319.

Bradley, D. F., and Felsenfeld, G. (1959), *Nature 185*, 1920.

Bradley, D. F., and Wolf, M. K. (1959), *Proc. Natl. Acad. Sci. U. S. 45*, 944.

Davies, J., Gilbert, W., and Gorini, L. (1964), *Proc. Natl. Acad. Sci. U. S. 51*, 883.

DeVoe, H., and Tinoco, I., Jr. (1962), *J. Mol. Biol. 4*, 518.

Feder, N., and Wolf, M. K. (1965), *J. Cell Biol. 27*, 327.

Furano, A. V. (1966), *J. Biol. Chem. 241*, 2237.

Geisser, S., and Bradley, D. F. (1962), *Bull. Inst. Intern. Statist. 39*, 269.

Hall, B. D., and Doty, P. (1959), *J. Mol. Biol. 1*, 111.

Klug, A., Holmes, K. C., and Finch, J. T. (1961), *J. Mol. Biol. 3*, 87.

Kurland, C. G. (1960), *J. Mol. Biol. 2*, 83.

Lamm, M. E., Childers, L., and Wolf, M. K. (1965), *J. Cell. Biol. 27*, 313.

Littauer, U. Z., and Eisenberg, H. (1959), *Biochim. Biophys. Acta 32*, 320.

Morgan, R. A., and Rhoads, D. J. (1965), *Biochim. Biophys. Acta 102*, 311.

Nash, H., and Bradley, D. F. (1965), *Biopolymers 3*, 261.

Pestka, S., Marshall, R., and Nirenberg, M. (1965), *Proc. Natl. Acad. Sci. U. S. 53*, 639.

Schlessinger, D. (1960), *J. Mol. Biol. 2*, 92.

Schneider, W. C. (1957), *Methods Enzymol. 3*, 680.

So, A. G., Bodley, J. W., and Davie, E. W. (1964), *Biochemistry 3*, 1977.

Spyrides, G. J., and Lipman, F. (1962), *Proc. Natl. Acad. Sci. U. S. 48*, 1977.

Stone, A. L., and Bradley, D. F. (1961), *J. Am. Chem. Soc. 83*, 3627.

Stone, A., Childers, L., and Bradley, D. (1963), *Biopolymers 1*, 111.

Szer, W., and Ochoa, S. (1964), *J. Mol. Biol. 8*, 823.

Tinoco, I., Jr. (1960), *J. Am. Chem. Soc. 82*, 4785.

Tissiers, A., Watson, J. D., Schlessinger, D., and Hollingworth, B. R. (1959), *J. Mol. Biol. 1*, 221.

von Ehrenstein, G., and Lipman, F. (1963), *Proc. Natl. Acad. Sci. U. S. 47*, 941.

Wettstein, F. O., Staehlin, T., and Noll, N. (1963), *Nature 197*, 430.

Zamenhof, S. (1957), *Methods Enzymol. 3*, 696.

Zubay, G., and Wilkins, M. H. F. (1960), *J. Mol. Biol. 2*, 105.